



Synergistic flame retardancy of aqueous hybridization between iron phosphonate and ammonium polyphosphate towards polyethyleneimine-based foam

Liehong Luo¹ · Weifeng Liu¹ · Liqing Zhai¹ · Wei Xie² · Lin Gan¹ · Hualin Wang² · Jin Huang¹ · Changhua Liu¹

Received: 14 November 2019 / Accepted: 8 February 2020 / Published online: 22 February 2020
© Iran Polymer and Petrochemical Institute 2020

Abstract

A hybrid flame retardant, of excellent stability in aqueous media, was designed to develop flame-retarded polyethyleneimine (PEI) foam. In this case, iron phosphonate (FeP) with carboxyl group and hydroxyl group was first designed and synthesized. The carboxyl group could be hydrogen bonded with the water-soluble ammonium polyphosphate (APP) in aqueous media, and then dispersed as nano-sized particles. Subsequently, the well-dispersed nano-hybrid of FeP and APP (FeP/APP) was blended with hydrophilic PEI to prepare a kind of composite foam through a freeze-drying process. For FeP/APP, the transition metal iron showed excellent catalytic carbonization performances. Meanwhile, APP could also catalyze the degradation of polymers to form a protective char layer. The thermogravimetric analysis coupled with Fourier transform infrared analysis (TG-FTIR) test disclosed that the improvement of flame retardancy for PEI-based foams was ascribed to the synergistic effect of FeP and APP in the condensed phase. The composite foam containing 30 wt% FeP/APP could self-extinguish and reach V-1 rating in UL-94 test. When the loading level of 45% FeP/APP reached 45%, the composite foam could elevate up to V-0 rating, and the peak of heat release rate and total heat release were reduced by 71.8% and 74.2%, respectively, compared to a neat PEI foam. It is worth noting that our work presents a promising way for preparation of stable aqueous flame retardant, and is expected to enhance the fire safety of aqueous foams, coatings, cotton textiles, and other flammable materials.

Keywords Iron phosphonate · Hybridization · Synergistic effect · Flame retardancy · Aqueous dispersion

Introduction

Polymer-based foams have been widely used in applications as furniture, automotive cushions, construction, etc., due to their high resilience, high heat insulations, and low densities

[1–3]. However, non-fire-retarded foams are highly flammable in the air. During the fire, these foams would generate a large amount of toxic smoke, which causes danger of burns and suffocation [4]. A simple and effective method to endow polymer-based foams with flame retardancy is to incorporate addition-type additives [5]. Various addition-type flame retardants, such as the ones with halogen, phosphorus, nitrogen, silicon, and sulfur content have been widely reported [6, 7]. Unfortunately, these flame retardants are usually insoluble or poorly dispersed in solvents. Therefore, the defects of poor compatibility, reduced mechanical properties, and easy leaching are inevitable during the process of use.

Solvent-dissolution/dispersed flame retardants are researched to solve these defects of solid additives. It can achieve better compatibility with the polymer matrix in the liquid phase [8, 9]. But to the best of our knowledge, many solvent-dissolution/dispersed flame retardants can only be dispersed in organic solvents rather than dispersed in aqueous solution. Besides, the extensive use of organic solvents will endanger human health and environmental safety [10].

Electronic supplementary material The online version of this article (<https://doi.org/10.1007/s13726-020-00792-x>) contains supplementary material, which is available to authorized users.

✉ Jin Huang
huangjin2015@swu.edu.cn

✉ Changhua Liu
chliu@swu.edu.cn

¹ School of Chemistry and Chemical Engineering, and Chongqing Key Laboratory of Soft-Matter Material Chemistry and Function Manufacturing, Southwest University, Chongqing 400715, People's Republic of China

² The First Scientific Research Institute of Wuxi, Wuxi 214035, People's Republic of China

Thus, it is an urgent need to develop a class of green, non-toxic water-dispersed flame retardants to solve these negative effects on human and the environment.

The aqueous foaming process enables a water-dispersed flame retardant to be well miscible with the polymer matrix to prepare flame-retarded polymer-based foam. Until now, there are only a limited number of reports on foamable hydrophilic polymer. Among them, polyethyleneimine (PEI), as a hydrophilic polymer, can dissolve in aqueous solution. The structure of multi-amino groups in PEI imparts its unique properties and extremely high chemical reactivity. It has been reported that PEI has high efficiency of CO₂ capture and smoke suppression performance as a flame retardant additive [11, 12]. Based on these advantages mentioned above, using PEI as a foam material will broaden its practical applications in the polymer field. However, the neat PEI foam itself is flammable and has a low compressive strength [13]. The research has shown that the addition of silica at above 80% can make the PEI foam exhibit excellent flame retardancy [14].

Ammonium polyphosphate (APP), as an acid source of traditional intumescent flame retardant, is considered to be an effective “green” fire retardant [15]. The low molecular weight APP is soluble in aqueous solution. APP is usually converted into polyphosphoric acid during the combustion process, when the protective carbonaceous layers are formed by catalytic dehydration of polyphosphoric acid [16]. However, the materials often exhibit limited flame retardancy when the APP was only added. The synergistic effect of phosphorous with transition metal compounds is a viable proposal to devise efficient flame retardants to achieve the flame retardant standard [16].

Transition metal phosphonate comprises an important segment in the market of nano synergists. It is the derivative of inorganic phosphate whose –OH group is substituted by an organic group. Transition metal ions as Lewis acids are reported to have superior catalytic carbonization performances, which can produce continuous and solid carbonaceous inorganic layer in combustion [17, 18]. In addition, the inorganic phosphate ceramic body produced by thermal degradation has high thermal stability and a low coefficient of thermal expansion which can enhance the stability of the flame retardant char layer [19]. Most importantly, the organic group not only participates in the construction of catalytic active sites, but also as a surface modifier to regulate its surface properties [20]. It has also proved that metal phosphonate containing Fe, Cu, Ce, Zr, and Zn exhibits special mechanical properties and flame resistance in composites [21, 22]. Therefore, it is expected

that the aqueous dispersion of the organic phosphonate can be achieved by regulating its surface groups.

Based on the above results, in this work, we proposed a strategy to prepare an efficient flame retardant hybrid that is very stable in aqueous media. Iron phosphonate (FeP) with carboxyl group and hydroxyl group was first designed and synthesized. The carboxyl group could be hydrogen bonded with the amino group of a water-soluble ammonium polyphosphate (APP); therefore, achieved its nano-dispersability in aqueous system. Subsequently, the stable aqueous suspension (FeP/APP) was combined with hydrophilic PEI in environmentally friendly water media to prepare a kind of flame-retarded composite foams. The synergistic catalytic carbonization performances between transition metal iron and APP made the PEI composite foams to exhibit prominent flame retardancy. The morphology, thermal stability, and combustion behavior of PEI-based foams were investigated in detail. Meanwhile, the flame-retarded mechanism was disclosed by the thermogravimetric analysis coupled with Fourier transform infrared analysis (TG-FTIR) test.

Experimental

Materials

Polyethyleneimine (PEI, 50% aqueous solution, branched polymer with M_w 750,000) was purchased from Zhengzhou Alpha Chemical Co., China. Ammonium polyphosphate (APP, short chain, water soluble) was provided by Zhenjiang Star Flame Retardant Technology Co., China. 2-Hydroxyphosphonoacetic acid was purchased from Shanghai Tengzhun Biotechnology Co., China. Ferric hydroxide was provided by Shanghai Titan Scientific Co., China, and the cross-linker (1,4-butanediol diglycidyl ether) was supplied by Tianjin Seanshop Technology Co., China.

Synthesis of FeP

FeP was synthesized by hydrothermal reaction of ferric hydroxide with 2-hydroxyphosphonoacetic acid. In summary, ferric hydroxide (0.04 mol) was dispersed in 120 mL de-ionized water under sonication for 30 min. Then, 2-hydroxyphosphonoacetic acid (0.04 mol) was added into the above mixture and stirred overnight. After that, the mixed solution was transferred to a Teflon-lined stainless steel autoclave and reacted at 160 °C for 48 h. The resultant precipitate was washed by de-ionized water, and oven dried at 60 °C for 12 h.

The hybridization of FeP and APP

The mass ratio of FeP and APP was fixed at 1:10. Briefly, FeP solid (1.0 g) was dispersed in 80 mL de-ionized water under stirring at 70 °C for 30 min. Meanwhile, APP solution, containing 10.0 g dissolved in 170 mL de-ionized water, was added dropwise into the above suspension. The stable colloidal dispersion was obtained after continuing the reaction for 8 h.

Preparation of the composite foams

A series of FeP/APP/PEI composite foams were prepared by one-step freeze-drying process. Briefly, FeP/APP colloidal dispersion was mixed with 2 g PEI (50% aqueous solution) and stirred to form a transparent solution. Then, 1 g cross-linker (1,4-butanediol diglycidyl ether) was added into the above solution to obtain the hydrogel under agitation. Subsequently, we allowed 24 h for the cross-linking reaction to be completed, and the hydrogel was frozen at -20 °C, freeze-dried for another 48 h for ice sublimation to obtain the target foam. Similarly, the FeP(45%)/PEI and APP(45%)/PEI foams were prepared without the addition of FeP and APP, respectively.

Characterization

Fourier-transform infrared spectroscopy (FTIR) was conducted on a Nicolet 170SX Fourier-transform infrared spectrometer (Madison, WI, USA) using KBr disc method.

Thermogravimetric analysis (TGA) was obtained using a TA-STDQ600 (New Castle, USA) instrument under nitrogen flow (20 mL/min). The samples were heated from 50 °C to 800 °C at a linear rate of 20 °C/min.

The morphology of the composite foams and char residues was observed using a scanning electron microscopy (JSM-6510LV, Japan). The samples were fractured in liquid nitrogen, and the fracture surfaces were later coated with a conductive platinum layer before observation. Transmission electron microscopy (TEM, JEM2100F, Japan) was used to study the structure of FeP, APP, and FeP/APP.

The apparent density of the composite foams was calculated by measuring its weight using an analytical balance and its volume by a digital caliper. The density, as the ratio of weight to volume, was measured three times on each sample to obtain an average value.

Elemental analysis for FeP was measured by Elementar Vario Micro Select (Germany).

Compression tests were performed using a Microelectronics Universal Testing Instrument Model Sans 6500 (Shenzhen, China) with a compression strain rate at 10 mm/min.

Three cylindrical samples (1 cm in diameter and 2 cm in height) were tested for each composition, and their values were averaged.

Raman spectrum of char residues was conducted on a Raman spectroscopy (Invia, Renishaw, Gloucestershire, UK) with a 532 nm laser source.

Thermogravimetric analysis coupled with Fourier transform infrared analysis (TG-FTIR) test was performed by a Pyris 1 thermogravimetric analyzer (Perkin-Elmer, USA) coupled with a Nicolet 6700 Fourier-transform infrared (Thermo Fisher Scientific Inc., USA) spectrophotometer through a polytetrafluoroethylene pipe. The samples were heated from 35 to 800 °C at a heating rate of 20 °C/min.

Vertical burning tests were performed with a CZF-3 vertical burning tester (Nanjing, China), similar to UL-94. The cylindrical foam samples with the height and diameter of 3 cm and 2 cm were used. The bottom of the samples was exposed to the flame for 10 s, and then the Bunsen burner was removed.

Limiting oxygen index (LOI) tests were measured on an oxygen index meter (ZR-01, Qingdao Shanfang Instrument Co., China), which was performed according to the ASTM D2863-2009.

The cone calorimetric test (CCT) was conducted on a cone calorimeter (6810, Suzhou Vouch Testing Technology Co., China) according to the ISO-5660 standard. The samples with the dimension of 100 mm × 100 mm were exposed to a radiant cone of 35 kW/m² heat flux.

Results and discussion

Structure and morphology of FeP/APP

The FTIR spectra of FeP, APP, and FeP/APP are shown in Fig. S1a. The peak of FeP at 3354 cm⁻¹ corresponded to the symmetrical hydroxyl-group stretch, and the peak at 1064 cm⁻¹ was the vibration absorption of Fe–OP groups [23]. These results indicated that the ferric hydroxide reacted with 2-hydroxyphosphonoacetic acid to form a Fe–OP bond. Moreover, the characteristic peaks of FeP at 1160 and 1635 cm⁻¹ corresponded to P=O and C=O stretching vibrations, respectively. This confirmed that FeP has been successfully synthesized. In comparison, for FeP/APP, all typical peaks of FeP and APP still exist, a red shift of the peak (–NH) from 3249 to 3222 cm⁻¹ indicated the existence of hydrogen bonds between FeP and APP [24]. In addition, for a series of FeP/APP/PEI composite foams (Fig. S1b), apart from the characteristic peak of PEI, the appearance of Fe–OP (1062 cm⁻¹) and P–O (905 cm⁻¹) indicated that the FeP/APP has been introduced into the PEI matrix.

Elemental analysis showed that the carbon and hydrogen contents of FeP were 11.2% and 1.9%, respectively.

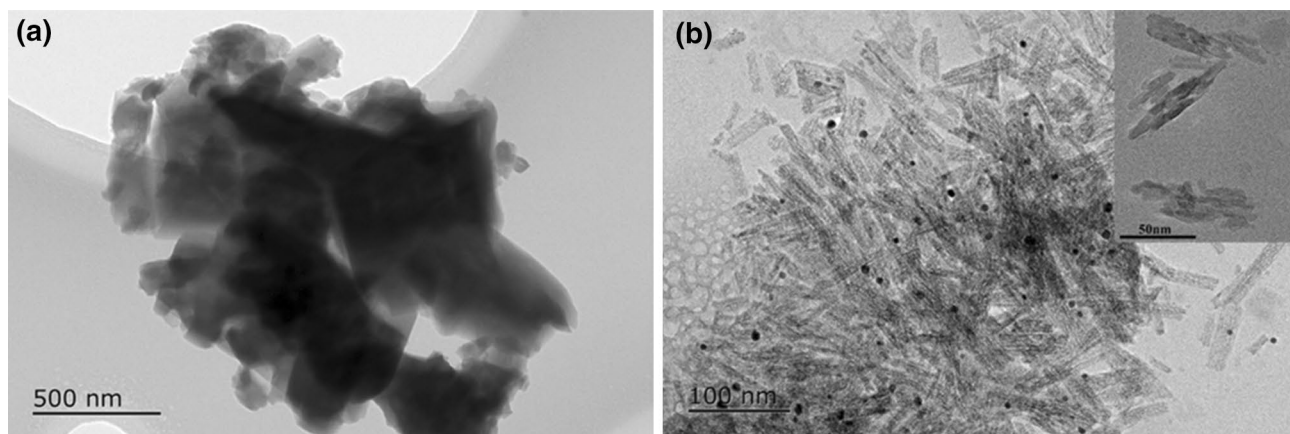
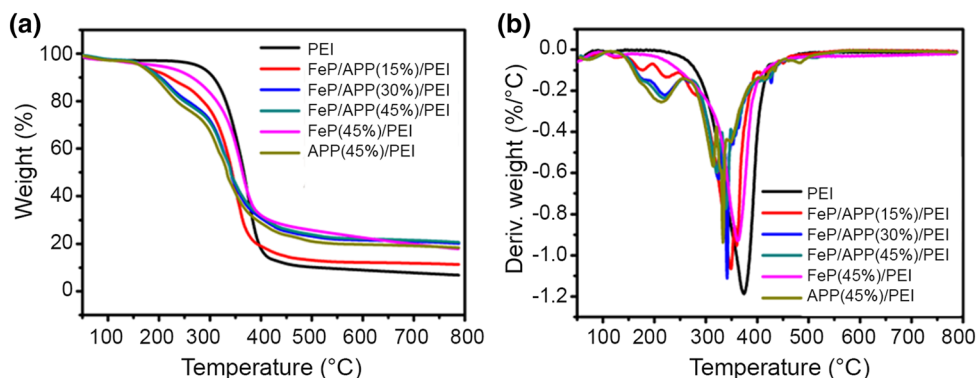


Fig. 1 TEM images of: **a** FeP, **b** FeP/APP, and APP (embedded figure in **b**)

Fig. 2 **a** TGA and **b** DTG curves of neat PEI and FeP/APP/PEI composite foams



Combined with TG experimental data (Fig. S1c), the molecular formula of the synthesized FeP was $\text{Fe}_2[\text{PO}_3\text{CH}(\text{OH})\text{COOH}]_3 \cdot 1.5\text{H}_2\text{O}$. The first mass loss before 200 °C was mainly the dehydration of FeP. The second weight loss occurred at 266 °C, associating with the release of 8.3% (its theoretical value at 8.5%). This was attributed to the dehydroxylation process in the aliphatic chain of FeP. The maximum mass loss was observed at 386 °C, which corresponded to the formation of ferric phosphate after removal of the carboxyl group (theoretical value was 20.9%). The total weight loss of organic matter (32.9%) was close to the theoretical value of 33.8%. This indicated that the organic part of the product has been decomposed to a great extent.

The morphology and structure of FeP, FeP/APP, and APP were observed by TEM. It is clear that FeP (Fig. 1a) displayed a nanosheet layer structure with obvious agglomeration. As for FeP/APP colloidal dispersion (Fig. 1b), the small black spots were FeP, and the long strips were APP (figure inset in Fig. 1b). It could be seen that FeP was dispersed into nano-sized particles with a size of about 5 nm.

Table 1 Data of the TGA curves for neat PEI and FeP/APP/PEI composite foams

Sample	$T_{5\%}$ (°C)	T_{max} (°C)	Residue (800 °C, wt%)
PEI	276	372	6.8
FeP/APP(15%)/PEI	166	349	11.4
FeP/APP(30%)/PEI	169	341	20.2
FeP/APP(45%)/PEI	170	339	20.8
FeP(45%)/PEI	193	362	17.9
APP(45%)/PEI	163	334	18.4

Thermal stability of PEI-based foams

To understand the effects of FeP/APP on FeP/APP/PEI composite foams, the thermal analyses (TG) of the neat PEI and flame retardant PEI composite foams were carried out (Fig. 2), and the related data are listed in Table 1. Neat PEI foam underwent one-stage degradation. It started to decompose at 276 °C ($T_{5\%}$, defined as the temperature at which

5% mass loss occurs), and T_{\max} (the temperature at the rate of maximum decomposition) occurred at 372 °C. Furthermore, the $T_{5\%}$ and T_{\max} of composite foams were lower than that of neat PEI foam. This was mainly the decomposition of APP prior to neat PEI foam. The ammonia and water released by the early degradation of APP could dilute the combustible gas, and also take away part of the heat from the system. These are beneficial to alleviate the burning of composites [25]. Meanwhile, the addition of APP, FeP, and FeP/APP obviously increased the residue weight at 800 °C, indicating the good catalytic charring ability of APP, FeP, and FeP/APP. The FeP/APP(45%)/PEI showed the highest residue, which was ascribed to the excellent synergistic effect between FeP and APP [26].

Apparent density and microstructure of the PEI-based foams

The related data of apparent density are listed in Table S1. All PEI-based foams exhibited similar densities with around 0.2 g/cm³. Also, the SEM micrographs of composite foams are shown in Figs. 3 and S2. APP-only foam exhibited a flat, collapsed cellular structure (Figs. S2a and S2b). Further, the cellular structure of FeP(45%)/PEI (Figs. S2c and S2d)

was irregular and uneven, it could be clearly seen that there were many agglomerated FeP in the pore and pore walls due to poor dispersion. When FeP/APP was added, the cellular structure of FeP/APP(45%)/PEI foam became more ordered, denser, and smaller with a pore size of about 100 microns, it was apparent that many secondary pores appeared on the pores well (Fig. 3a, b). These results indicated that the FeP/APP could facilitate the formation of cell structure through the strong interfacial interaction among FeP, APP, and PEI. Moreover, the strong deformation resistance of small cells accounts for the increase of compression modulus for composite foams [27].

To further confirm the dispersion of FeP/APP in FeP/APP(45%)/PEI foam, the energy dispersive spectroscopy (EDS) elemental mapping of P and Fe distributions in the selected region (Fig. 3b) are displayed in Fig. 3c, d, respectively. The Fe and P elements were homogeneously dispersed in foam with no aggregates observed. This indicated that FeP/APP was uniformly distributed in PEI foam.

Combustion behavior of PEI-based foams

Vertical burning test is a kind of effective method to evaluate the combustion performance of composite foams. The

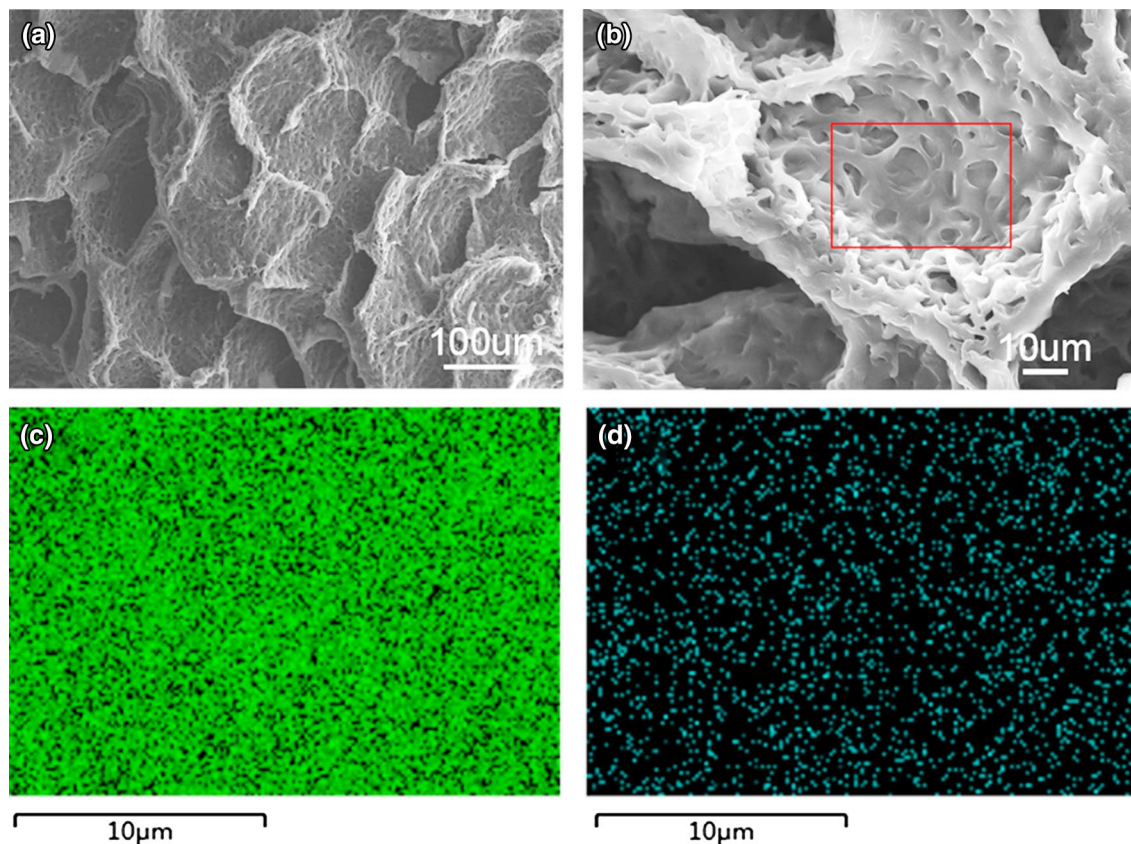


Fig. 3 SEM images of a–b FeP/APP(45%)/PEI foam and elemental mappings of c phosphorus and d iron for the selected region in b

Table 2 The UL-94 rating, and LOI results of neat PEI and PEI-based composite foams

Sample	UL-94			Rating	LOI (%)
	t_1 (s)	t_2 (s)	Dripping		
PEI	> 30	/	No	NR	17.4±0.2
FeP/APP(15%)/PEI	> 30	/	No	NR	25.6±0.3
FeP/APP(30%)/PEI	26	5	No	V-1	28.5±0.2
FeP(45%)/PEI	> 30	/	No	NR	19.5±0.4
APP(45%)/PEI	22	10	No	V-1	20.0±0.3
FeP/APP(45%)/PEI	6	1	No	V-0	31.8±0.2

results are listed in Table 2 and the digital photos are shown in Fig. S3. The neat PEI foam exhibited no rating in UL-94 vertical burning test. It is easy to ignite and burn rather quickly until it is burned out with almost no residual char remaining. In contrast, the FeP/APP composite foams exhibited excellent flame retardancy as the FeP/APP load increases, i.e. FeP/APP(30%)/PEI could self-extinguish and reach V-1 in UL-94 test, and FeP/APP(45%)/PEI foam could pass UL-94V-0, which was due to the efficient synergy between nano-size FeP and APP, thus achieving high-efficiency flame retardancy. Interestingly, no dripping was also observed during the combustion of all samples including neat PEI foam, which means that PEI has great potential to replace other traditional polymer-based foams.

Limiting oxygen index (LOI) measurements were carried out to evaluate the combustion performance of composite foams. The corresponding values are summarized in Table 2. With the increase of FeP/APP loading, the LOI values of composite foams increased from 17.4% for neat PEI to 25.6%, 28.5%, and 31.8% for FeP/APP(15%)/PEI, FeP/APP(30%)/PEI, and FeP/APP(45%)/PEI, respectively, which implied these foams are self-extinguishable in air. However, foam with only added FeP or APP showed a slight increase in the LOI value. The result indicated that the significant improvement of flame retardancy for

FeP/APP foams was due to an excellent synergistic effect between FeP and APP.

To further evaluate the synergistic influence between FeP and APP on the flame retardancy of PEI quantitatively, E_{pppms} was used to calculate the synergistic effect index of FeP/APP(45%)/PEI foam [13].

$$E_{pppms} = \frac{(\text{LOI}_{\text{FeP/APP(45\%)/PEI}} - \text{LOI}_{\text{PEI}})}{[(\text{LOI}_{\text{FeP(45\%)/PEI}} - \text{LOI}_{\text{PEI}}) + (\text{LOI}_{\text{APP(45\%)/PEI}} - \text{LOI}_{\text{PEI}})]}$$

The synergistic effect is reflected in $E_{pppms} > 0$, and the antagonistic effect is $E_{pppms} < 0$. The value of E_{pppms} was 3, indicating an obvious synergistic effect between FeP and APP.

The fire-retardant behavior of PEI composite foams was further evaluated by the cone calorimetric test (CCT). The heat release rate (HRR), total heat release (THR) curves of PEI composite foams are shown in Figs. 4a, 4b, and the corresponding data are summarized in Table 3. Neat PEI foam burned very quickly after ignition with a peak heat release rate (pHRR) of 819 kW/m². The pHRR of FeP(45%)/PEI, APP(45%)/PEI, and FeP/APP(45%)/PEI were 478, 258, and 231 kW/m², in the stated order. The lowest pHRR was achieved by FeP/APP(45%)/PEI, with a remarkable decrease in pHRR (71.8%). Besides, the THR of composite foams gradually decreased and the FeP/APP(45%)/PEI foam gave rise to the lowest THR, nearly 74.2% reduction compared with that of neat PEI foam. These results were ascribed to the excellent catalytic char ring properties of FeP and APP. FeP and APP showed an obvious synergistic effect, which promoted the formation of a more stable intumescent char layer. The fire growth rate (FGR) was used to assess the fire hazard of composites according to the following equation [28]:

$$\text{FGR} = \text{pHRR}/t_{\text{pHRR}}$$

Generally, a lower FGR represents that the time to flash over was delayed. The FGR of FeP/APP(45%) was 3.8 kW/

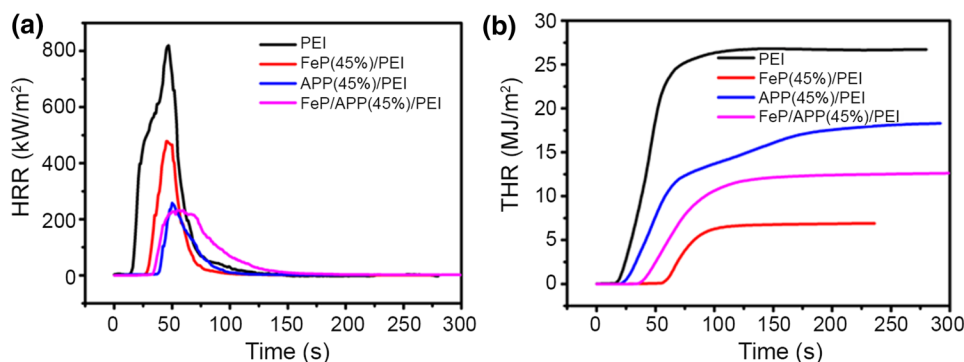
Fig. 4 The curves of: **a** HRR and **b** THR of neat PEI and composite foams

Table 3 Combustion parameters obtained from the cone calorimeter test

Sample	PEI	FeP(45%)/PEI	APP(45%)/PEI	FeP/APP(45%)/PEI
pHRR (kW/m ²)	819 ± 16	478 ± 11	258 ± 10	231 ± 8
tPHRR (s)	47 ± 2	46 ± 1	50 ± 2	61 ± 1
FGR (kW/m ² s)	17.4 ± 1.2	10.4 ± 0.5	5.2 ± 0.4	3.8 ± 0.2
THR (MJ/m ²)	26.7 ± 2.1	18.3 ± 1.8	12.6 ± 2.0	6.9 ± 1.5
pSPR (m ² /s)	0.037 ± 0.001	0.048 ± 0.002	0.065 ± 0.001	0.021 ± 0.001
TSP (m ²)	0.80 ± 0.03	0.90 ± 0.02	1.19 ± 0.01	0.28 ± 0.03
pCOP (g/s)	0.018 ± 0.001	0.007 ± 0.001	0.006 ± 0.002	0.002 ± 0.001
pCO ₂ P (g/s)	0.35 ± 0.01	0.23 ± 0.03	0.09 ± 0.03	0.10 ± 0.01
Residue (wt%)	2.6 ± 0.1	10.0 ± 0.1	18.6 ± 0.1	23.4 ± 0.1

m²s, reducing about 78.2%, indicating the FeP/APP has superior flame retardant properties for PEI foam.

The parameters of smoke production rate (SPR), total smoke production (TSP), carbon monoxide production (COP), and carbon dioxide production (CO₂P) are also summarized in Table 3, and the curves of CO and CO₂ are shown in Fig. S4a, b. Noticeably, the addition of APP could not lower the SPR and TSP. However, for FeP/APP(45%)/PEI, the peak smoke production rate (pSPR) and TSP obviously declined to 0.021 m²/s and 0.28 m², further to confirm the synergistic effect between FeP and APP. Besides, with the introduction of FeP/APP, the peak carbon monoxide production (pCOP) and peak carbon dioxide production (pCO₂P) greatly decreased to 0.002 g/s and 0.10 g/s, reducing to about 88% and 71.4%, respectively. These results were attributed to that the organic skeleton of PEI was more catalyzed to remain in the condensed phase rather than being converted to volatile gases for further combustion [12, 29]. Correspondingly, the FeP/APP(45%)/PEI also showed the highest char residues (23.4%), much higher than that of neat PEI foam (2.6%).

Flame retardant mechanism of FeP/APP

Analysis of char residues

To better understand the flame retardant mechanism, the char residues of PEI-based composites after the LOI test were analyzed by the SEM test and Raman spectroscopy. The morphologies of char residues were investigated by SEM in Fig. S5. The residual char of neat PEI (Fig. S5a), FeP(45%)/PEI (Fig. S5b), and APP(45%)/PEI (Fig. S5c) looked relatively fragile, with many obvious no-uniform voids and folds, which failed to prevent the flame and heat transfer. Whereas the char from FeP/APP(45%)/PEI (Fig. S5d) foam was more continuous and more compact, which was due to the excellent synergistic effect between FeP and APP. The decomposed products of FeP and APP catalyzed degradation of PEI in the condensed phase to form a more stable char. The stable char could act as a superior barrier for both heat

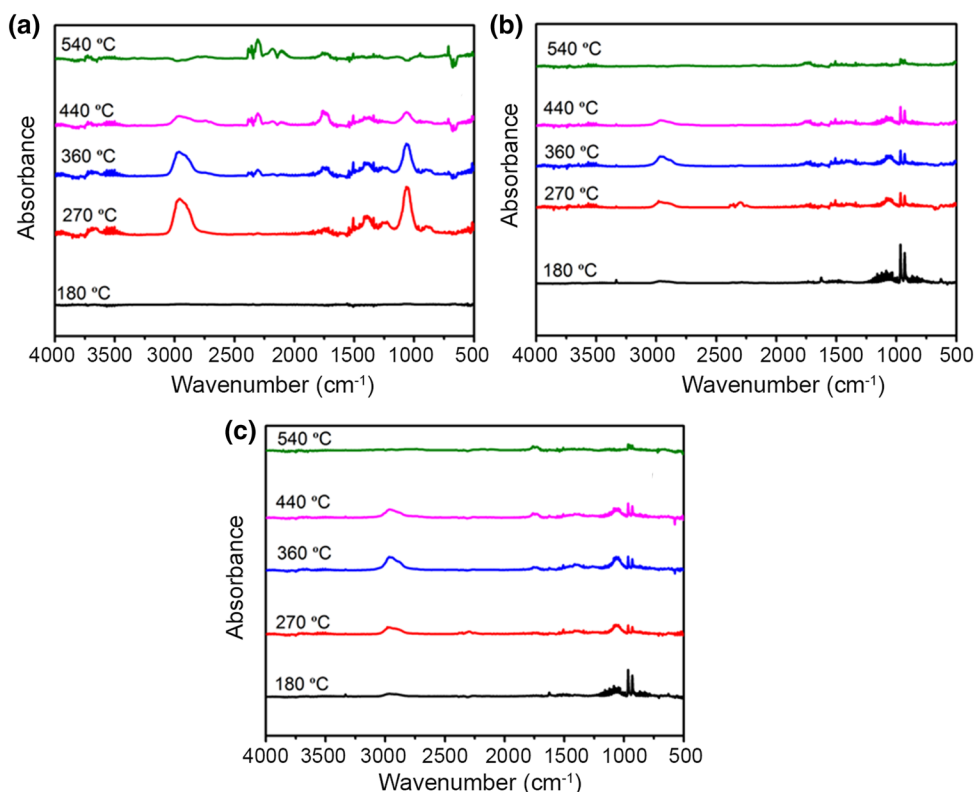
flow and gas transport, thus preventing the further combustion of the underlying material [30].

The Raman spectra of char residues after the LOI test are shown in Fig. S6. There are two main bands, located at approximately 1590 (G band) and 1370 cm⁻¹ (D band). The former corresponded to the first-order scattering of the E_{2g} phonon of sp² C atoms, whereas the latter represented the activation in the first-order scattering process of sp³ carbons and the presence of defect-like amorphous domains [21, 32]. The intensity ratio of D-band to G-band (*I_D/I_G*) was used to indicate the graphitization degree of the char residue. Interestingly, from neat PEI (1.76) to FeP(45%)/PEI (1.67), APP(45%)/PEI (1.42), then to FeP/APP(45%)/PEI (1.16), the *I_D/I_G* of composite foams gradually decreased, indicating the improvement of the degree of graphitization in residual char. The high-quality char layer tended to better protect inner materials from thermal degradation by preventing the volatile flammable gases from being exposed to heat and oxygen.

Evolved gas analysis

To investigate the flame retardant mechanism of FeP/APP in the gas phase, TG-FTIR was used to analyze the pyrolysis products during the entire pyrolysis process under a nitrogen atmosphere, with the results are shown in Fig. 5. The characteristic peaks in neat PEI foam (Fig. 5a) at 2965, 1736, 2336, 2180, and 1080 cm⁻¹ corresponded to the absorbance of hydrocarbons, carbonyl compounds, CO₂, CO, and ether, respectively [33]. Furthermore, its main degradation was between 270 and 360 °C and the releases of CO₂ and CO were mainly after 360 °C. However, all the characteristic peaks mentioned above were significantly weakened in APP(45%)/PEI (Fig. 5b) and FeP/APP(45%)/PEI foam (Fig. 5c), and were also consistent with the reduction of smoke, CO₂, CO in CCT test. No characteristic peaks containing phosphorus were found. It could be inferred that the addition of APP, FeP/APP obviously inhibited the pyrolysis of PEI. They catalyzed more gaseous products to participate in the char formation process, thereby increasing the char

Fig. 5 FTIR spectra for the condensed products of: **a** neat PEI foam, **b** APP(45%)/PEI foam, and **c** FeP/APP(45%)/PEI foam at different temperatures



yield in the condensed phase, rather than exerting a flame retardant effect in the gas phase. Moreover, a comparison of the infrared absorption intensity versus time of the main products of neat PEI, APP(45%)/PEI, and FeP/APP(45%)/PEI foam are qualitatively shown in Fig. S7. The maximum absorption of pyrolysis products in FeP/APP(45%)/PEI was less than that of the APP(45%)/PEI and neat PEI. These results indicated that the hybridization of FeP and APP could further enhance the catalytic char formation efficiency, leading to a significant reduction of releasing flammable volatile species, and a decrease in pHRR and THR.

On the basis of the condensed phase and gas phase analysis, possible flame retardant mechanisms of composite foams are proposed in Fig. S8. The excellent flame retardant property of FeP/APP/PEI was mainly attributed to the superior condensed phase flame-retarded effect. The decomposed products of FeP and APP synergistically catalyzed and induced the formation of carbonaceous residue. Then, a more compact and higher degree of graphitization protective layer was created, which acted as a barrier to prevent the migration of heat and gases.

Compressive behavior of PEI-based foams

The compressive properties of composite foams are shown in Fig. S9, and the related data of compressive properties are listed in Table S1. The compressive strength of FeP/APP/

PEI composite foams gradually increased with the increase of FeP/APP content. For example, the stress at 50% strain of the FeP/APP(45%)/PEI composite foam (719.4 kPa) was much higher than that of the neat PEI foam (6.6 kPa). Also, the compressive modulus of FeP/APP/PEI composite foams exhibited a similar trend with the compressive stress. Compared with the neat PEI foam (8.46 kPa), the FeP/APP(45%)/PEI composite foam showed the highest compressive modulus (1229.3 kPa). These significant improvements in mechanical properties were primarily related to the composition and cellular structure of foams. First, the FeP nanoparticles itself acted as a good reinforcing agent in polymers to enhance the strength and modulus [34]. Second, due to the interaction of FeP/APP with PEI, incorporating FeP/APP into PEI tended to form a denser and smaller cellular structure. Obviously, this could enhance the ability of the foam to resist deformation [27]. Therefore, the composites exhibited excellent compression modulus. In contrast, the addition of FeP or APP alone did not achieve such a high reinforcing effect.

Conclusion

In summary, we proposed a strategy to prepare flame retardants that are well-stable in aqueous media. The hybrid flame retardant (FeP/APP) was obtained by hydrogen bonding

between iron phosphonate (FeP) and ammonium polyphosphate (APP). Subsequently, the aqueous suspension of the FeP/APP hybrid was blended with hydrophilic polyethyleneimine (PEI) to construct flame-retarded composite foam through the freeze-drying process. The limiting oxygen index (LOI) and vertical burning test presented that 30 wt% FeP/APP addition could cause foam self-extinguish, and 45 wt% FeP/APP was a suitable amount to achieve V-0 rating and 31.8% in LOI. The cone calorimeter test (CCT) results gave further evidence that the incorporation of FeP/APP could dramatically decrease the fire growth rate (FGR), heat release rate (HRR), total release rate (THR), production of smoke, and simultaneously enhance the yield of the residual char. For FeP/APP composite foams, transition metal ions presented prominent catalytic carbonization performances, and APP could also catalyze the degradation of polymers to form a protective char layer. The study on the flame-retardant mechanism towards PEI-based foam was mainly derived from the synergistic effect between FeP and APP in the condensed phase. Thermogravimetric analysis also demonstrated that the residual yields of FeP/APP/PEI were improved. This high-efficiency flame retardant foam prepared by a green, facile method was a promising alternative to conventional polymer-based foams.

Acknowledgments This research is financially supported by the Project for Chongqing University Innovation Research Group of Chongqing Education Committee (CXQT19008), and the Chongqing Talent Plan for Innovation and Entrepreneurship Demonstration Team (CQYC201903243).

References

- Rao W, Xu H, Xu Y, Qi M, Liao W, Xu S, Wang Y (2018) Persistently flame-retardant flexible polyurethane foams by a novel phosphorus-containing polyol. *Chem Eng J* 343:198–206
- Qian L, Feng F, Tang S (2014) Bi-phase flame-retardant effect of hexa-phenoxy cyclotriphosphazene on rigid polyurethane foams containing expandable graphite. *Polymer* 55:95–101
- Patrick J, Sottos N, White S (2012) Microvascular based self-healing polymeric foam. *Polymer* 53:4231–4240
- McKenna S, Hull T (2016) The fire toxicity of polyurethane foams. *Fire Sci Rev* 5:1–27
- Xu W, Wang G, Zheng X (2015) Research on highly flame-retardant rigid PU foams by combination of nanostructured additives and phosphorus flame retardants. *Polym Degrad Stab* 111:142–150
- Wu N, Niu F, Lang W, Xia M (2019) Highly efficient flame-retardant and low-smoke-toxicity poly(vinyl alcohol)/alginate/montmorillonite composite aerogels by two-step crosslinking strategy. *Carbohydr Polym* 221:221–230
- Laufer G, Kirkland C, Morgan A, Grunlan J (2013) Exceptionally flame retardant sulfur-based multilayer nanocoating for polyurethane prepared from aqueous polyelectrolyte solutions. *ACS Macro Lett* 2:361–365
- Chen H, Shen P, Chen M, Zhao H, Schiraldi D (2016) Highly efficient flame retardant polyurethane foam with alginate/clay aerogel coating. *ACS Appl Mater Interf* 8:32557–32564
- Cheng X, Tang R, Yao F, Yang X (2019) Flame retardant coating of wool fabric with phytic acid/polyethyleneimine polyelectrolyte complex. *Prog Org Coat* 132:336–342
- Costes L, Laoutid F, Brohez S, Dubois P (2017) Bio-based flame retardants: when nature meets fire protection. *Mater Sci Eng R* 117:1–25
- Cheng J, Liu N, Hu L, Li Y, Wang Y, Zhou J (2019) Polyethyleneimine entwine thermally-treated Zn/Co zeolitic imidazolate frameworks to enhance CO₂ adsorption. *Chem Eng J* 364:530–540
- Cai W, Hong N, Feng X, Zeng W, Shi Y, Zhang Y, Wang B, Hu Y (2017) A facile strategy to simultaneously exfoliate and functionalize boron nitride nanosheets via Lewis acid-base interaction. *Chem Eng J* 330:309–321
- Guo X, Zhao L, Zhang L, Li J (2012) Surface modification of magnesium aluminum hydroxide nanoparticles with poly(methyl methacrylate) via one-pot in situ polymerization. *Appl Surf Sci* 258:2404–2409
- Chatterjee S, Shanmuganathan K, Kumaraswamy G (2017) Fire-retardant, self-extinguishing inorganic/polymer composite memory foams. *ACS Appl Mater Interf* 9:44864–44872
- Zhang J, Kong Q, Wang D (2018) Simultaneously improving the fire safety and mechanical properties of epoxy resin with Fe-CNTs via large-scale preparation. *J Mater Chem A* 6:6376–6386
- Kong Q, Sun Y, Zhang C, Guan H, Zhang J, Wang D, Zhang F (2019) Ultrathin iron phenyl phosphonate nanosheets with appropriate thermal stability for improving fire safety in epoxy. *Compos Sci Technol* 182:107748
- Zhang J, Kong Q, Yang L, Wang D (2016) Few layered Co(OH)₂ ultrathin nanosheet-based polyurethane nanocomposites with reduced fire hazard: from ecofriendly flame retardance to sustainable recycling. *Green Chem* 18:3066–3074
- Chen X, Jiang Y, Jiao C (2014) Smoke suppression properties of ferrite yellow on flame retardant thermoplastic polyurethane based on ammonium polyphosphate. *J Hazard Mater* 266:114–121
- Kong Q, Wu T, Zhang J, Wang D (2018) Simultaneously improving flame retardancy and dynamic mechanical properties of epoxy resin nanocomposites through layered copper phenylphosphate. *Compos Sci Technol* 154:136–144
- Natarajan S, Mandal S (2010) Open-framework structures of transition-metal compounds. *Angew Chem* 47:4798–4828
- Ran S, Guo Z, Chen C, Zhao L, Fang Z (2014) Carbon nanotube bridged cerium phenylphosphonate hybrids, fabrication and their effects on the thermal stability and flame retardancy of the HDPE/BFR composite. *J Mater Chem A* 2:2999–3007
- Chen C, Guo Z, Ran S, Fang Z (2014) Synthesis of cerium phenylphosphonate and its synergistic flame retardant effect with decabromodiphenyl oxide in glass-fiber reinforced poly(ethylene terephthalate). *Polym Compos* 35:539–547
- Huang Y, Yang Y, Ma J, Yang J (2018) Preparation of ferric phosphonate/phosphinate and their special action on flame retardancy of epoxy resin. *J Appl Polym Sci* 135:46206
- Wang L, Wu S, Dong X, Wang R, Zhang L, Wang J, Zhong J, Wu L, Wang X (2018) A pre-constructed graphene-ammonium polyphosphate aerogel (GAPPA) for efficiently enhancing the mechanical and fire-safety performances of polymers. *J Mater Chem A* 6:4449–4457
- Chang T, Shen W, Chiu Y, Ho S (1995) Thermo-oxidative degradation of phosphorus-containing polyurethane. *Polym Degrad Stab* 49:353–360
- Zhang W, He X, Song T, Jiao Q, Yang R (2014) The influence of the phosphorus based flame retardant on the flame retardancy of the epoxy resins. *Polym Degrad Stab* 109:209–217

27. Xu T, Zhang C, Li P, Dai X, Qu L, Sui Y, Gu J, Dou Y (2018) Preparation of dual-functionalized graphene oxide for the improvement of the thermal stability and flame-retardant properties of polysiloxane foam. *New J Chem* 42:13873–13883
28. Shao Z, Deng C, Tan Y, Chen M, Chen L, Wang Y (2014) An efficient mono component polymeric intumescent flame retardant for polypropylene: preparation and application. *ACS Appl Mater Interf* 6:7363–7370
29. Guo W, Wang X, Zhang P, Liu J, Song L, Hu Y (2018) Nanofibrillated cellulose-hydroxyapatite based composite foams with excellent fire resistance. *Carbohydr Polym* 195:71–78
30. Wang Y, Yang X, Peng H, Wang F, Liu X, Yang Y, Hao J (2016) Layer-by-layer assembly of multifunctional flame retardant based on Brucite, 3-aminopropyltriethoxysilane, and alginate and its applications in ethylene-vinyl acetate resin. *ACS Appl Mater Interf* 8:9925–9935
31. Zhao B, Chen L, Long J, Jian R, Wang D (2013) Synergistic effect between aluminum hypophosphite and alkyl-substituted phosphinate in flame-retarded polyamide 6. *Ind Eng Chem Res* 52:17162–17170
32. Xia Y, Jin F, Mao Z, Guan Y, Zheng A (2014) Effects of ammonium polyphosphate to pentaerythritol ratio on composition and properties of carbonaceous foam deriving from intumescent flame-retardant polypropylene. *Polym Degrad Stab* 107:64–73
33. Shen Y, Gong W, Zheng B, Meng X, Gao L (2016) Synergistic effect of Ni-based bimetallic catalyst with intumescent flame retardant on flame retardancy and thermal stability of polypropylene. *Polym Degrad Stab* 129:114–124
34. Zhou S, Zheng X, Yu X, Wang J, Weng J, Li X, Feng B, Yin M (2007) Hydrogen bonding interaction of poly(D, L-lactide)/hydroxyapatite nanocomposites. *Chem Mater* 19:247–253